arXiv:2302.12343v1 [cs.CL] 23 Feb 2023

CHiLL: Zero-shot Custom Interpretable Feature Extraction from Clinical Notes with Large Language Models

Denis Jered McInerney MCINERNEY.DE@NORTHEASTERN.EDU
Northeastern University, Boston, MA

Geoffrey Young GSYOUNG@BWH.HARVARD.EDU
Brigham and Women's Hospital, Boston, MA

Jan-Willem van de Meent J.W.VANDEMEENT@UVA.NL
University of Amsterdam, Netherlands

Byron C. Wallace B.WALLACE@NORTHEASTERN.EDU
Northeastern University, Boston, MA

Abstract

Large Language Models (LLMs) have yielded fast and dramatic progress in NLP, and now offer strong *few-* and *zero-shot* capabilities on new tasks, reducing the need for annotation. This is especially exciting for the medical domain, in which supervision is often scant and expensive. At the same time, model predictions are rarely so accurate that they can be trusted blindly. Clinicians therefore tend to favor "interpretable" classifiers over opaque LLMs. For example, risk prediction tools are often linear models defined over manually crafted predictors that must be laboriously extracted from EHRs. We propose **CHiLL (Crafting High-Level Latents)**, which uses LLMs to permit *natural language specification of high-level features for linear models* via zero-shot feature extraction using expert-composed queries. This approach has the promise to empower physicians to use their domain expertise to craft features which are clinically meaningful for a downstream task of interest, without having to manually extract these from raw EHR (as often done now). We are motivated by a real-world risk prediction task, but as a reproducible proxy, we use MIMIC-III and MIMIC-CXR data and standard predictive tasks (e.g., 30-day readmission) to evaluate our approach. We find that linear models using automatically extracted features are comparably performant to models using reference features, and provide greater interpretability than linear models using "Bag-of-Words" features. We verify that learned feature weights align well with clinical expectations.

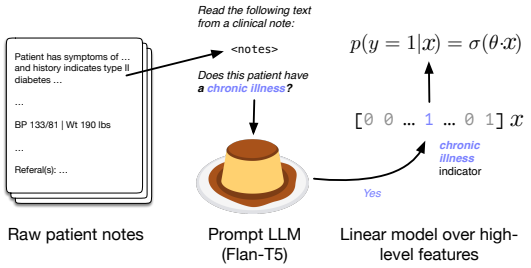

Figure 1: We propose to allow domain experts to specify high-level features for simple linear predictive models in natural language, and then extract these *zero-shot* (without supervision) using large language models.

1. Introduction

Statistical models for clinical tasks often rely on data that is weakly informative of the prediction target. For this reason, model predictions can rarely be taken at face value and practitioners have a natural preference for simple models defined over interpretable predictors (features), in contrast to deep models that operate over dense learned representations. We focus on linear models specifically so that predictors are associated with weights; this simplicity permits inspection of weights to ensure clinical tenability and may mitigate undesired fragilities exhibited by highly parameterized large neural models.

A downside to relying on interpretable features is that one often has to manually *extract* them from patient records. This can be particularly difficult when

© D.J. McInerney, G. Young, J.-W.v.d. Meent & B.C. Wallace.

features are more abstract, and may need to be inferred from unstructured (free-text) fields within the EHR. Recent work (Agrawal et al., 2022) has shown that large language models (LLMs) are capable *zero-shot* extractors of clinical information, i.e., they can extract structured information from records without explicitly being trained to do so.

In this work we investigate the potential of zero-shot extraction *for definition and abstraction of interpretable features from unstructured EHR to use as inputs for simple (linear) models* (Figure 1). These can be high-level features specified in natural language and so are more interpretable than low-level features such as Bag-of-Words (BoW) representations. The basic motivation of this work is to evaluate the approach of instantiating small linear models defined over high-level features automatically extracted via LLMs—without explicit supervision—from unstructured data in EHR.

A practical security and privacy concern that arises in healthcare is that we cannot send off sensitive patient data to the OpenAI GPT-3 (Brown et al., 2020) API. This is because patient data is protected by HIPPA, which precludes such data use. Even publicly available deidentified EHR data such as MIMIC (Johnson et al., 2016b) have terms which forbid this. In this work we show that despite the specialized domain, Flan-T5 (Chung et al., 2022; Wei et al., 2022) variants—which can fit on a single GPU and run locally—can perform zero-shot feature extraction from EHR with reasonable accuracy.

Our contributions are summarized as follows:

- We propose and evaluate a method for extracting high-level interpretable features from clinical texts using Flan-T5 given corresponding prompts, and we evaluate the how well these extracted features align with ground truth.
- We demonstrate that we can capitalize on the calibration of the LLM to improve performance, such that using extracted features performs comparably to using the reference features.
- We show that the resulting linear models' weights align with clinician-annotated notions of how features should impact a prediction.
- We investigate the data- and feature- efficiency of our approach and find that it can achieve similar results with much less data and utilizes features efficiently.

Our hope is that this work is a step toward capitalizing on the strong inference capabilities of LLMs in settings where interpretability is paramount. The promising preliminary results we report suggest several avenues for further exploration, e.g., modeling correlations between inferred features, probing the degree to which such predictors provide useful and reliable interpretability, and modifying trained linear models directly based on expert judgement.

2. Methods

We consider binary classification of patients on the basis of free text from their EHR data. A now standard approach to such tasks would entail adopting a neural language encoder E to induce a fixed-length d-dimensional distributed representation of an input x—e.g., the `[CLS]` embedding in BERT (Devlin et al., 2018; Alsentzer et al., 2019) models—and feeding this forward to a linear classification head to yield a logit:

$$p(y = 1 \mid x) = \sigma\big(w^T E_{[\texttt{CLS}]}(x)\big) \tag{1}$$

where $y \in \{0, 1\}$, $x \in \mathbb{R}^{L \times V}$, and $w \in \mathbb{R}^d$. (For BERT, $d = 768$.) However, a downside to this approach is that it is not amenable to inspection; the prediction is made on the basis of a dense learned representation from a pre-trained network, and it is unclear which patient attributes give rise to the prediction. A simpler and (at least arguably) more interpretable approach is to use a linear model defined over Bag-of-Words (BoW) representations:

$$p^{\text{BoW}}(y = 1|x) = \sigma(w^T x^{\text{BoW}}). \tag{2}$$

This approach is more interpretable in that it operates over (transformations of) token counts, and therefore the learned w has a natural correspondence to words in the vocabulary. Linear models that operate over tens of thousands of word predictors occupy an intermediate space between the interpretability afforded by simpler, smaller models defined over high-level features and neural models which use opaque representations. For some clinical tasks, however, BoW with large vocabularies can be competitive with respect to downstream performance.

Instruction-tuned LLMs offer the opportunity to use LLMs without any finetuning to predict targets, but we use them to instead infer intermediate, high-level, features $f \in \mathbb{R}^N$ using N expert-specified prompt templates $t_1, ..., t_N$:

$$f_n^{\text{binary}} = \mathbb{I}[\text{argmax}_z(\text{LLM}(z|t_n(x))) = v_{\text{yes}}] \tag{3}$$

where $t_n(x)$ denotes the prompt obtained by populating the template t_n with x, z represents the next token after the prompt and v_{yes} represents the index of the token "yes" in the vocabulary. We then use a simple linear model over these predicted features to predict the target.

$$p(y = 1) = \exp\left(w^T \cdot f^{\text{binary}}\right) \tag{4}$$

where $w \in \mathbb{R}^N$.

Predictions from the LLM for the high-level binary features will be imperfect, and are naturally associated with a confidence under the LLM: The probability of the token "yes" normalized by the mass assigned to *either* "yes" or "no". As a simple means of incorporating uncertainty in extracted features, we can use this continuous value in place of binary feature indicators. For feature n (elicited using template t_n) we have:

$$f_n^{\text{cont}} = \frac{\text{LLM}(z = v_{\text{yes}}|t_n(x))}{\text{LLM}(z = v_{\text{yes}}|t_n(x)) + \text{LLM}(z = v_{\text{no}}|t_n(x))} \tag{5}$$

3. Evaluation

To evaluate the proposed approach, we consider four tasks. We use the MIMIC-III corpus (Johnson et al., 2016b,a; Goldberger et al., 2000) to permit reproducibility. We first consider standard clinical predictive tasks in MIMIC (Section 3.1): Readmission, mortality, and phenotype prediction. For these we treat ICD codes as proxies for high-level features.[1] This allows us to evaluate the accuracy of the zero-shot extraction component, and to compare the performance of a linear model defined over the true ICD codes as compared to the same model when operating over inferred features.

We then consider X-ray report classification using the MIMIC-CXR dataset (Johnson et al. 2019b,a,c; Johnson et al.; Goldberger et al. 2000; Section 3.2). In this case we elicit queries for intermediate feature descriptions from a radiologist co-author that they believed *a priori* would be relevant to the report classification categories defined in CheXpert (e.g., "Does this patient have a normal cardiac silhouette?"; see Appendix Table A for all examples). This demonstrates the flexibility of the approach—and the promise of allowing domain experts to specify features in natural language—but we are limited in our ability to evaluate the extraction performance directly in this case.

3.1. Clinical predictive tasks on MIMIC-III

For the three standard clinical prediction tasks we consider, we use ICD codes as proxies for high-level, interpretable features that one might want to infer. While somewhat contrived, this setup allows us to evaluate how well the inferred features agree with the "true" features (i.e., ICD-code indicators). We use the top 10 most frequent ICD codes in the training set as features.[2] To demonstrate the flexibility of the approach, we also consider two custom features which one might expect to be informative: (1) Does the patient have a chronic illness? (2) Is the condition life-threatening?

Readmission prediction For 30-day readmission, we follow the task definition, setup, and data preprocessing outlined in Huang et al. (2019).

In-hospital Mortality prediction This task involves predicting whether a patient will pass during a particular stay in the hospital given the notes from the first 48 hours of that stay. We adapt our preprocessing code for this task from Zhang et al. (2020).

Phenotype prediction Zhang et al. (2020) also derive various phenotypes from medical records using ICD codes, using these to define a phenotype prediction task which we also consider in this work. (We again adapt their preprocessing code for this task.)

3.2. Chest X-ray report classification

We next consider chest X-ray report classification. This allows us to draw upon the expertise of a practicing radiologist co-author. We use the MIMIC-CXR dataset (Johnson et al., 2019b,a,c; Johnson et al.; Goldberger et al., 2000) with CheXpert labels (Irvin et al., 2019)—again to ensure reproducibility—and evaluate performance on a 12-label classification task.

Given that these labels can be automatically derived, the predictive task considered here is not in and of itself practically useful, but it provides an illustrative example with which to explore the potential

1. In practice one could of course use ICD codes directly as predictors. We are using this setup as an exemplary task using publicly available data to demonstrate the potential of the proposed approach in a way that also allows us to compare to models which have access to "ground-truth" high-level features, i.e., the ICD codes.

2. In preliminary experiments we found that including >10 ICD codes as predictors in linear models did not appreciably improve AUROC for the three tasks considered.

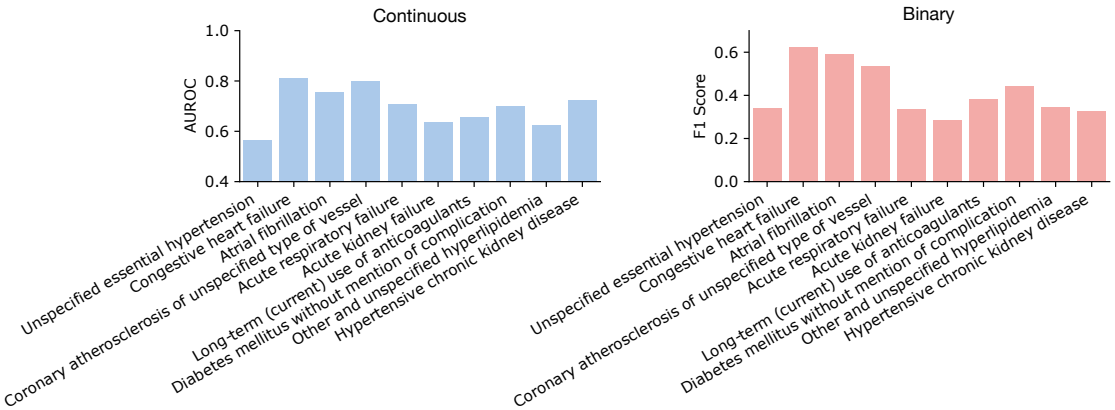

Figure 2: Feature extraction performance on the readmission prediction task. AUROC for continuous ICD code features (left) and F1 for binary ICD code features (right), compared to reference ICD codes. (Note that these results would compare unfavorably to fine-tuned ICD code prediction models, given that we are assuming a zero-shot setting.)

power of allowing domain experts (here, a radiologist) to craft bespoke features for a given task. We use outputs of the CheXpert automated report labeler as "labels". We omit two downstream labels from our results—Consolidation and Pleural Effusion—because we included these as intermediate features instead under the advisement of our radiologist co-author.[3] (The names of the 12 labels we predict are shown in Table 2.)

To infer intermediate features, we asked a radiologist team-member (and co-author on this work) to provide natural binary questions they would ask to categorize radiology reports into the given classes (Appendix A). We refer to these questions as queries, and use them as prompts for the LLM to extract corresponding indicators (or probabilities) for each of these. In this case, because these are truly novel predictors specified by a domain expert, we do not have "reference" features to compare to (as we did above where we treated ICD codes as high-level features). However, in Section 4.3 a domain expert assesses the degree to which learned coefficients for features align with clinical judgement.

3.3. Experimental details

To extract features, we use Flan-T5-XXL (Roberts et al., 2022) with fp16 enabled (for speed) on a Quadro RTX 8000 with 46G of memory. To fit logistic regression models, we use the `sklearn` (Pedregosa et al., 2011) package's `SGDClassifier` with the logistic loss and the the default settings (this includes adding an intercept and an $\ell 2$ penalty).

3. We did use these extra two labels in training, but this only affects BERT, which was trained in a 'multi-task' way with a shared encoder used (and updated) across all labels. We think it unlikely that this would impact performance much.

4. Results

We aim to address the following research questions empirically.

Feature extraction (4.1) How *accurate* are zero-shot extracted features, as compared to reference (manually extracted) predictors?

Downstream classification performance (4.2) How does classification based on exper our approach compare to black box and simple models on the ultimate downstream classification?

Interpretability (4.3) Do the inferred features permit intuitive interpretation, and do the resultant coefficients align with clinical expectations?

Data- and Feature- efficiency (4.4) Do these features offer additional benefits in terms of data and/or feature efficiency?

We address each of these questions in turn.

4.1. Feature extraction

We first measure the accuracy of automatically inferred high-level features. In the case of ICD-code proxy features, we can evaluate this directly using the actual ICD codes as reference labels with which to calculate Precision, Recall, and F1 scores for binary features, and AUROC for our continuous fea-

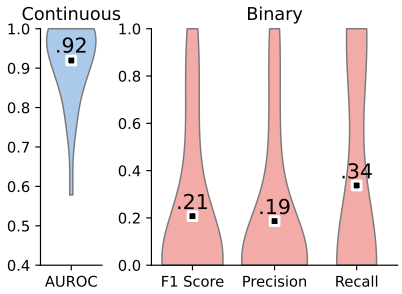

Figure 3: Feature inference performance on annotated Chest X-ray data. Histograms are over features. For continuous feature AUROCs, we omit features that do not have any positive labels in the 50 annotated examples. For F1 of binary features, we omit features that correspond to ill-defined precision (no positive predictions) and/or recall (no positive labels) scores are set to 0.

tures (although we cannot do this for the two custom, non-ICD code features considered). We present these metrics for the readmission task in Figure 2.

For the radiology task, we have no reference features to use for evaluation. Therefore, our radiologist co-author annotated 50 test example reports with a set of features applicable to each report. This allows us to create binary labels for each feature and report, in turn allowing evaluation with the same metrics used above for binary and continuous feature encodings. There are 105 features—too many to present individually—so we report the feature scores in violin plots (Figure 3).

Zero-shot (feature) extraction performs reasonably well here in general, as suggested by prior work (Agrawal et al. 2022; although they used GPT-3, not Flan-T5). A novel aspect of this work, in contrast to (Agrawal et al., 2022), is that in the case of the chest X-ray task *the features are extracted using custom queries, specified as natural language questions provided by a domain expert (radiologist)*. While far from perfect, our results suggest that modern large instruction-tuned LMs are capable of inferring arbitrary clinically salient high-level features from EHR with some fidelity.

4.2. Downstream classification performance

Classification performance in and of itself is not our primary objective; rather, our aim is to design a method which allows for flexible construction of small and interpretable models using high-level features, with minimal expert annotation effort. Nonetheless, to contextualize the predictive performance of the models evaluated here we also consider several baseline models which offer varying degrees of "interpretability". Specifically, we compare against fine-tuned variants of (a) Clinical BERT (Alsentzer et al., 2019), and (b) a logistic regression model defined over BoW (TF-IDF) features with varying vocabulary sizes. AUROC for Phenotyping and Chest X-ray report classification are averaged over the labels.

To evaluate the degree to which zero-shot inference degrades performance due to inaccurate feature extraction, we also report results for a logistic regression model defined over *reference* ICD codes ("Ground Truth") for the MIMIC tasks considered. As a final point of reference, we compare against direct zero-shot prediction of the *downstream classification* using Flan-T5-XXL (Roberts et al., 2022).

Figure 4[4] demonstrates that across all tasks, the model variants with continuous intermediate features have significant signal (i.e., AUROC is significantly above the chance 0.5). With that said, prediction on the downstream task based on these features performs worse than BERT and TF-IDF (30k) models. We also see that the addition of just the two expert queries improves performance across the board for the MIMIC-III tasks relative to models that solely employ ICD-code queries, indicating that there is indeed a benefit that can be derived from employing expert queries to predict intermediate features.

Zero-shot prediction of the downstream task performs worse than (supervised) linear models on top of inferred features on Readmission prediction and Chest X-ray report classification, on par with it on Phenotyping, and slightly better than it on Mortality prediction. However, such predictions are completely blackbox (see Section 5 for discussion of the interpretability implications of zero-shot extracted features.) Finally, we also find that using binary features instead of continuous features degrades performance significantly (Table 1); calibrating (un)certainty helps.

When manually inspecting some example radiology reports, it became apparent that downstream labels

4. Expanded set of results in Apppendix Table B.1.

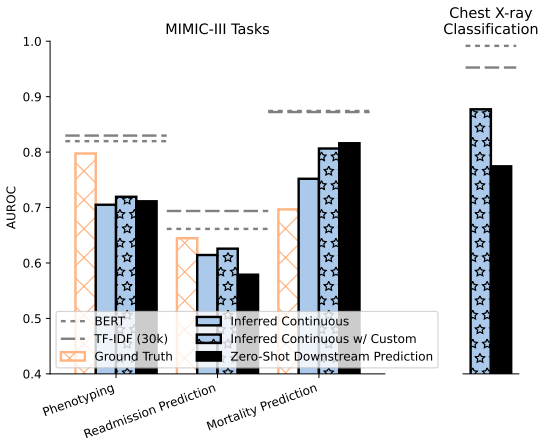

Figure 4: Downstream classification performance. We compare variants that use inferred continuous features with models that use "ground truth" features (here, ICD codes), and models that perform zero-shot prediction directly. For reference, we also show the performance of TF-IDF and BERT models (dashed horizontal lines).

are often verbalized in the radiology report. This makes sense given that the CheXpert labeler needs to extract these from the report, and intermediate features are therefore not explicitly modeled. This gives TF-IDF and BERT models a particular advantage over inferred feature models that is unlikely to exist for natural tasks (which are not defined by an automated labeler, and where intermediate features will probably be important.)

We also note that models that use ICD code features (inferred and especially real) have an advantage in Phenotyping because the phenotypes considered were derived from ICD codes, although the features used are a small subset of the ICD codes used to define the task. This explains why using the "ground truth" ICD code features do particularly well here.

w/ Custom	Pheno.	Readmis.	Mort.	CXR Class.
✗	-.054	-.025	-.052	-
✔	-.050	-.023	-.088	-.060

Table 1: Delta AUROC from using Binary Features instead of Continuous.

4.3. Interpretability

Given our primary motivation to offer "interpretability"—specifically, in the form of small linear models over a small number of high-level features—we next investigate how well learned coefficients align with domain expert judgement.

The radiologist who specified the features to be used for the chest X-ray dataset also indicated the for which task(s) they judged each feature to be predictive. Consequently, we have specified a label for each of the 105 features that indicates whether the domain expert believed the feature to be likely supportive of, or likely not relevant to, each of the 12 classes defined in the chest X-ray task.

We use these "feature labels" to measure the degree to which the learned weights agree with the domain knowledge that they are intended to encode. In particular, we rank each feature by coefficient and compute precision at k and AUC for all 12 classes (Table 2). For all labels except Lung Opacity and Support Devices, the rank of features in terms of relevance consistently agrees with expert judgement (AUC $> .5$).

To provide further evidence of the greater interpretability afforded by the proposed approach, compared to natural alternatives, we present plots of the top features for Readmission prediction (Figure 5). Here we compare the top-ranked features in linear models using TF-IDF (left), reference ICD codes (the "ground truth" high-level features here; center), and inferred high-level features (right). The top positive

	P@1	P@5	P@10	P@20	AUC
No Finding	1.00	0.40	0.20	0.10	0.62
Enlar. Cardiom.	1.00	0.20	0.10	0.05	1.00
Cardiomegaly	1.00	0.80	0.60	0.35	0.61
Edema	0.00	0.20	0.30	0.20	0.62
Pneumonia	0.00	0.20	0.20	0.10	0.64
Atelectasis	0.00	0.20	0.20	0.10	0.69
Pneumothorax	1.00	0.60	0.30	0.15	0.84
Fracture	1.00	0.40	0.30	0.15	0.74
Lung Lesion	0.00	0.60	0.40	0.25	0.80
Lung Opacity	0.00	0.00	0.00	0.00	0.29
Pleural Other	0.00	0.20	0.40	0.20	0.73
Support Devices	0.00	0.40	0.30	0.30	0.49
Average	0.42	0.35	0.27	0.16	0.67

Table 2: Precisions and AUCs of learned feature rankings in the Chest X-ray classification dataset, evaluated against *a priori* relevancy judgements per class provided by our radiologist collaborator.

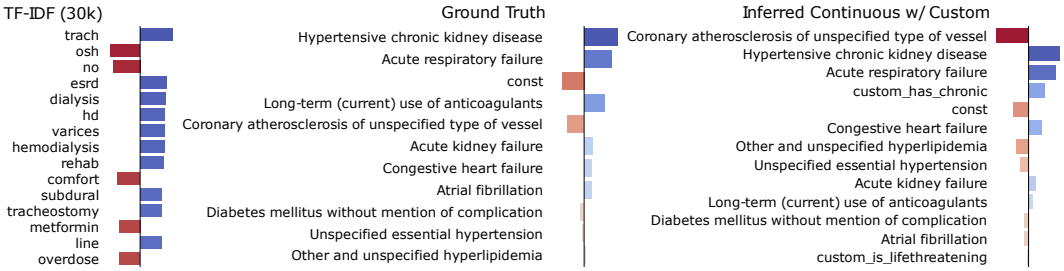

Figure 5: Linear model coefficients for readmission prediction. Blue and red indicate features that support or refute the label, respectively, and "const" refers to the values of the intercept.

inferred high-level features align with the top positive reference ICD code features.

For the high-level features, coefficient magnitude mass is concentrated on the very top features, whereas in the TF-IDF case the mass is more uniformly distributed. We find this to hold across many of the tasks and labels (see appendix Table B.2). This is likely an artifact of having many more TF-IDF features, but it makes such models more difficult to interpret. We also see that the custom "has_chronic" feature is among the top features and the "custom_is_lifethreatening" feature is at the bottom. This aligns with expectations for readmission prediction.

We also explore the coefficients for chest X-ray report classification, allowing our radiologist co-author to annotate these post-hoc. It is important to do this analysis post-hoc because the initial feature annotations used for the metrics in Table 2 are not necessarily exhaustive. Figure 6 reports assessments for the coefficients of the linear model for "atelectasis". Most of the feature influences agree with expectations.

Interestingly this analysis indicates the presence of certain types of known reporting biases present in the reports. For example, the feature "apical lucency" specifically indicates possible pneumothorax, which is a cause of passive atelectasis, and so rationally should support the 'atelectasis' label, but in fact is weighted to refute the label. We speculate that this reflects the well-known 'satisfaction of search' bias, and other closely aligned reporting biases; pneumothorax is such a critically important condition that radiologists reporting pneumothorax will in many cases not spend time searching for, or reporting the associated atelectasis, which in this case is a secondary feature of far lower independent importance.

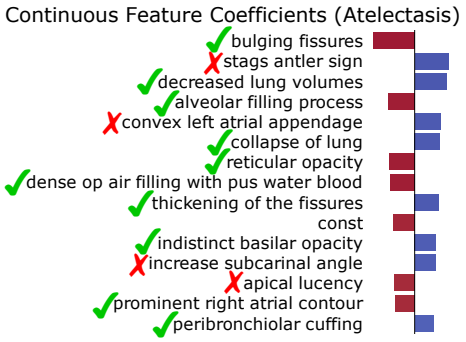

Figure 6: Linear model coefficients for predicting **Atelectasis** in the Chest X-ray Dataset using the continuous features. ✓ and ✗ denote post-hoc annotations of the feature coefficient as aligning or not aligning with expectations, respectively. Most do.

Figure 6 shows an example selected to illustrate how a clinician might inspect a classification. Because the predicted "edema" label was discordant with the CheXpert labeler, we asked our radiologist collaborator to review this case to determine which features incorrectly led to this ostensible "false positive". While inspecting the features for a source of error, our radiologist collaborator determined that the top positive features ("alveolar filling process" and "alveolar fluid") accurately describe the report, and can be supportive of Edema, but would more commonly reflect pneumonia or other causes. Subsequently, while reviewing the report, the radiologist concluded that **the model prediction of Edema was actually correct** and the CheXpert label represented a false negative. Here the model (correctly) did not predict pneumonia and did predict Edema, so

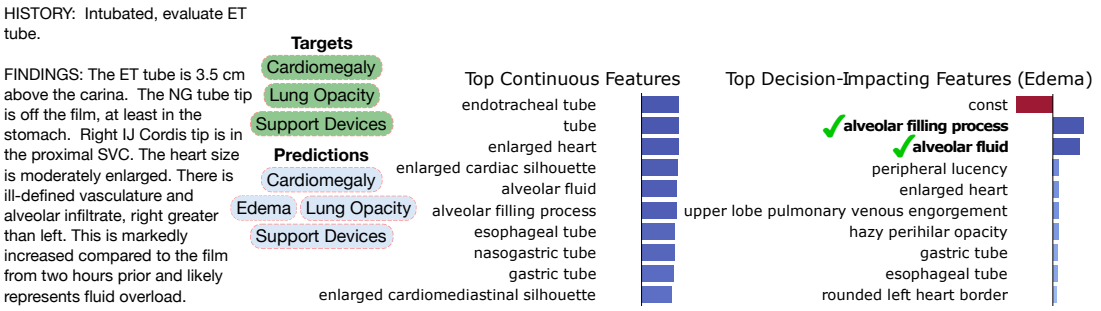

Figure 7: Qualitative example of features and feature influence for predicting Edema in the case of an ostensible "false positive". We selected this example because on cursory inspection Edema would seem to be applicable here. We presented this to our radiologist co-author who confirmed that ***this report should in fact be labeled positive for Edema***. We show the report and the downstream reference and predicted labels on the left. In the middle, we report top raw feature values, and on the right we show the top scores, i.e., feature values times the corresponding coefficients for Edema. **Bolded** features were confirmed by the radiologist as aligning with clinical judgement.

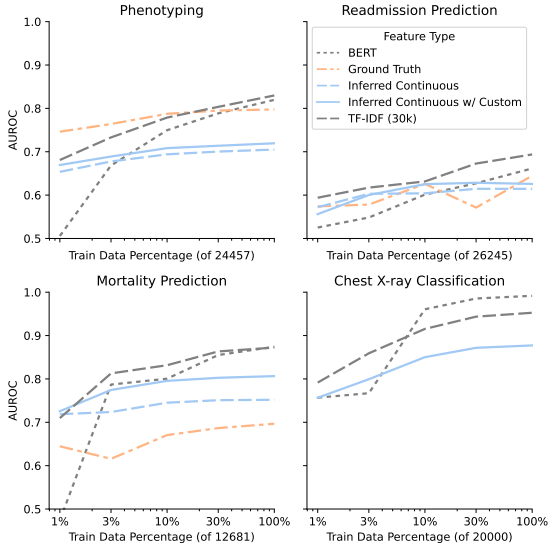

Figure 8: Learning curves for different methods.

the inferred features influenced the 'edema/no edema' binary decision correctly. Appendix Figure B.2 shows a different example where a feature influenced the model incorrectly, even though the model ultimately made the correct prediction. These examples illustrate two of many ways in which our approach might facilitate model interpretation and debugging.

4.4. Data- and feature- efficiency

Finally, we consider how our model fares compared to baselines in terms of data efficiency. Specifically, we construct learning curves by increasing the percent of the available data used to train models. In Figure 8, we see that the performance of small models plateaus with relatively minimal supervision. At low levels of supervision such models are competitive—and in some cases better than—larger models (e.g., based on Clinical BERT representations), which benefit more from additional supervision. We again emphasize, however, that using more complex representations comes at the expense of interpretability; this is true even for TF-IDF (see Figure 5).

We also explore the distribution of information among the features by pruning features from our continuous model after training in Figure 9. If we prune features randomly, we see a curve that indicates that we have not saturated our performance, and adding additional features will likely increase performance further. In fact, while annotating 50 examples on the test set, our radiologist co-author noted many features that were not included that would likely increase performance.

If we prune features with the smallest-magnitude coefficients first, we see that—in contrast to the model using binary features—the continuous feature model has a much more rounded curve, indicating that there are a large number of features that are actively contributing to a performance increase.

We also note that the number of features we infer is dramatically less than the number of features needed by TF-IDF. Indeed we see in the expanded results in the appendix (Table B.1) that if we limit TF-IDF to a vocabulary size of 100, the continuous features do

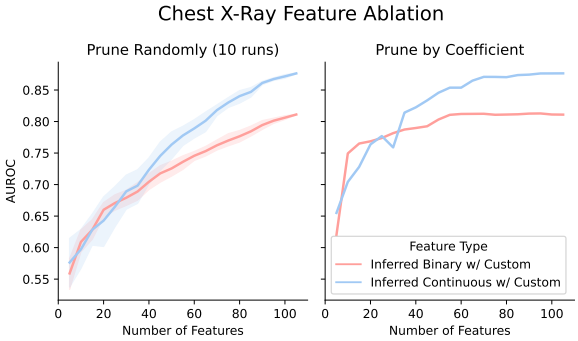

Figure 9: Ablation over number of features for Chest X-ray classification. After training, we explore how pruning features randomly (left) or based on coefficient magnitudes (averaged over all classes) affects performance.

beat TF-IDF across all tasks (though only slightly in the chest X-ray task).

5. Discussion and limitations

Small linear models operating over well-defined features offer a straightforward sort of transparency: One can read off coefficients for each predictor and inspect which features most influenced the output for a given instance (e.g., see Figure 7). This is in stark contrast to models defined as deep neural networks (like Clinical BERT; Alsentzer et al. 2019, and other deep neural encoders), which operate over dense learned embeddings. However, in healthcare, high-level features must often be manually extracted from unstructured EHR. The idea in this work is to allow domain experts to define high-level queries in natural language, infer the response automatically by prompting an LLM using these queries, and then define small linear models over the resulting features.

The promise of this approach is that it enables one to capitalize on LLMs while still building models that provide interpretability. Our approach allows domain experts to craft features that align with questions that a clinician might seek to answer in order to make a diagnosis and then use the coefficients from a trained linear model to determine which features inform predictions. Using such "abstract" features in place of word frequency predictors confers greater interpretability (Figure 5).

While the initial results reported in this paper are encouraging, they also raise many questions as to how one should design queries that will yield intermediate features that are interpretable, informative, and verifiable. One fundamental limitation of using LLMs to generate high-level features is that predictions for these features are still opaque. This suggests a few immediate research questions for future work:

The slippery "interpretability" of inferred features; Is there a trade-off between interpretability and predictive power? Not every query that is informative of the downstream prediction task will necessarily aid interpretability. For example, when predicting mortality, the response to the query *"Is the patient at risk of death?"* is likely to correlate strongly with the downstrean task; we have seen this in Figure 4, which shows that zero-shot queries can yield good predictive performance. At the same time, a query such as this one essentially paraphrases the original downstream task, which does little to aid interpretability. We have now simply shifted the problem to explaining what elements of the EHR give rise to the predicted "feature". This suggests that expert queries should yield individual features that correlate with the prediction task, yet are are also not strongly correlated with one another.

How do we know whether predicted features are faithful to their queries? A related complication to this approach is that zero-shot feature extraction will not be perfect. While results for ICD code proxies indicate good correlation, we will in general not be able to easily verify whether the indicator that is extracted by an LLM is in fact predicting the feature intended. The interpretability of the resultant model will therefore depend on the degree to which the LLM inferences align with the domain experts' intent regarding the respective features. This suggests that we might want to design queries for high-level features that, whenever possible, are easily verifiable upon inspection of the EHR. Asking if a patient is at risk of death is not directly verifiable, because it is necessarily a prediction; asking if the patient has an "enlarged heart" (for example) probably is. However, even using verifiable features does **not** guarantee that clinicians will hastily confirm or remain unbiased by unverified features in practice.

Can we manually intervene when a model learns a counter-intuitive dependency? Because we exploit features that have a direct relation-

ship to domain expert knowledge, it might be possible to draw upon their judgement to intervene when a model learns a dependence on a predictor in way that does not align with expectations (e.g. Figures 6 and B.2). This may happen because either: (1) the feature itself was incorrectly inferred, (2) there exists some spurious correlation in the data that does not hold in general. A less likely possibility is that (3) the expert prior was simply incorrect. Future work might study if pruning this feature to "correct" the model improves generalization.

6. Conclusions

We have proposed using large language models (LLMs) to infer high-level features from unstructured Electronic Health Records (EHRs) to be used as predictors in small linear models. These high-level features can be specified in arbitrary natural language queries composed by domain experts, and extracted using LLMs without explicit supervision.

On three clinical predictive tasks, we showed that this approach yields performance comparable to that achieved when using "reference" high-level features (here, ICD codes). On a fourth task (X-ray report classification), we enlisted a radiologist collaborator to provide high-level features in natural language. We showed a model using these features as automatically extracted via an LLM realized strong predictive performance, and—more importantly in our view—provided varieties of model transparency which we confirmed aligned with clinical judgement, and which provided insights to the domain expert.

This work demonstrates the promise of using LLMs as high-level feature extractors for small linear models, which may admit varieties of interpretability. However, this is complicated by the issues discussed in Section 5; more research into this hybrid approach is therefore warranted.

Acknowledgements

We acknowledge partial funding for this work by National Library of Medicine of the National Institutes of Health (NIH) under award numbers R01LM013772 and R01LM013891. The work was also supported in part by the National Science Foundation (NSF) grant 1901117. The content is solely the responsibility of the authors and does not necessarily represent the official views of the NIH or the NSF.

References

Monica Agrawal, Stefan Hegselmann, Hunter Lang, Yoon Kim, and David Sontag. Large language models are zero-shot clinical information extractors. In *Proceedings of Empirical Methods in Natural Language Processing (EMNLP)*, 2022.

Emily Alsentzer, John Murphy, William Boag, Wei-Hung Weng, Di Jin, Tristan Naumann, and Matthew McDermott. Publicly available clinical BERT embeddings. In *Proceedings of the 2nd Clinical Natural Language Processing Workshop*, pages 72–78, Minneapolis, Minnesota, USA, June 2019. Association for Computational Linguistics. doi: 10.18653/v1/W19-1909. URL https://www.aclweb.org/anthology/W19-1909.

Tom B. Brown, Benjamin Mann, Nick Ryder, Melanie Subbiah, Jared Kaplan, Prafulla Dhariwal, Arvind Neelakantan, Pranav Shyam, Girish Sastry, Amanda Askell, Sandhini Agarwal, Ariel Herbert-Voss, Gretchen Krueger, Tom Henighan, Rewon Child, Aditya Ramesh, Daniel M. Ziegler, Jeffrey Wu, Clemens Winter, Christopher Hesse, Mark Chen, Eric Sigler, Mateusz Litwin, Scott Gray, Benjamin Chess, Jack Clark, Christopher Berner, Sam McCandlish, Alec Radford, Ilya Sutskever, and Dario Amodei. Language models are few-shot learners. *CoRR*, abs/2005.14165, 2020. URL https://arxiv.org/abs/2005.14165.

Hyung Won Chung, Le Hou, Shayne Longpre, Barret Zoph, Yi Tay, William Fedus, Eric Li, Xuezhi Wang, Mostafa Dehghani, Siddhartha Brahma, et al. Scaling instruction-finetuned language models. *arXiv preprint arXiv:2210.11416*, 2022.

Jacob Devlin, Ming-Wei Chang, Kenton Lee, and Kristina Toutanova. Bert: Pre-training of deep bidirectional transformers for language understanding. *arXiv preprint arXiv:1810.04805*, 2018.

Ary L Goldberger, Luis AN Amaral, Leon Glass, Jeffrey M Hausdorff, Plamen Ch Ivanov, Roger G Mark, Joseph E Mietus, George B Moody, Chung-Kang Peng, and H Eugene Stanley. Physiobank, physiotoolkit, and physionet: components of a new research resource for complex physiologic signals. *circulation*, 101(23):e215–e220, 2000.

Kexin Huang, Jaan Altosaar, and Rajesh Ranganath. Clinicalbert: Modeling clinical notes and predicting hospital readmission. *arXiv:1904.05342*, 2019.

Jeremy Irvin, Pranav Rajpurkar, Michael Ko, Yifan Yu, Silviana Ciurea-Ilcus, Chris Chute, Henrik Marklund, Behzad Haghgoo, Robyn Ball, Katie Shpanskaya, et al. Chexpert: A large chest radiograph dataset with uncertainty labels and expert comparison. In *Proceedings of the AAAI conference on artificial intelligence*, volume 33, pages 590–597, 2019.

A Johnson, T Pollard, R Mark, S Berkowitz, and S Horng. Mimic-cxr database (version 2.0.0). physionet, 2019a.

Alistair Johnson, Matt Lungren, Yifan Peng, Zhiyong Lu, Roger Mark, Seth Berkowitz, and Steven Horng. Mimic-cxr-jpg-chest radiographs with structured labels.

Alistair E. W. Johnson, Tom J. Pollard, and Roger G. Mark. MIMIC-III clinical database (version 1.4), 2016a.

Alistair E. W. Johnson, Tom J. Pollard, Seth J. Berkowitz, Nathaniel R. Greenbaum, Matthew P. Lungren, Chih-ying Deng, Roger G. Mark, and Steven Horng. MIMIC-CXR, a de-identified publicly available database of chest radiographs with free-text reports. *Scientific Data*, 6(1):317, December 2019b. ISSN 2052-4463. doi: 10.1038/s41597-019-0322-0. URL https://doi.org/10.1038/s41597-019-0322-0.

Alistair E.W. Johnson, Tom J. Pollard, Lu Shen, Li-wei H. Lehman, Mengling Feng, Mohammad Ghassemi, Benjamin Moody, Peter Szolovits, Leo Anthony Celi, and Roger G. Mark. MIMIC-III, a freely accessible critical care database. *Scientific Data*, 3(1):160035, May 2016b. ISSN 2052-4463. doi: 10.1038/sdata.2016.35. URL https://doi.org/10.1038/sdata.2016.35.

Alistair EW Johnson, Tom J Pollard, Nathaniel R Greenbaum, Matthew P Lungren, Chih-ying Deng, Yifan Peng, Zhiyong Lu, Roger G Mark, Seth J Berkowitz, and Steven Horng. Mimic-cxr-jpg, a large publicly available database of labeled chest radiographs. *arXiv preprint arXiv:1901.07042*, 2019c.

F. Pedregosa, G. Varoquaux, A. Gramfort, V. Michel, B. Thirion, O. Grisel, M. Blondel, P. Prettenhofer, R. Weiss, V. Dubourg, J. Vanderplas, A. Passos, D. Cournapeau, M. Brucher, M. Perrot, and E. Duchesnay. Scikit-learn: Machine learning in Python. *Journal of Machine Learning Research*, 12:2825–2830, 2011.

Adam Roberts, Hyung Won Chung, Anselm Levskaya, Gaurav Mishra, James Bradbury, Daniel Andor, Sharan Narang, Brian Lester, Colin Gaffney, Afroz Mohiuddin, Curtis Hawthorne, Aitor Lewkowycz, Alex Salcianu, Marc van Zee, Jacob Austin, Sebastian Goodman, Livio Baldini Soares, Haitang Hu, Sasha Tsvyashchenko, Aakanksha Chowdhery, Jasmijn Bastings, Jannis Bulian, Xavier Garcia, Jianmo Ni, Andrew Chen, Kathleen Kenealy, Jonathan H. Clark, Stephan Lee, Dan Garrette, James Lee-Thorp, Colin Raffel, Noam Shazeer, Marvin Ritter, Maarten Bosma, Alexandre Passos, Jeremy Maitin-Shepard, Noah Fiedel, Mark Omernick, Brennan Saeta, Ryan Sepassi, Alexander Spiridonov, Joshua Newlan, and Andrea Gesmundo. Scaling up models and data with `t5x` and `seqio`. *arXiv preprint arXiv:2203.17189*, 2022. URL https://arxiv.org/abs/2203.17189.

Jason Wei, Maarten Paul Bosma, Vincent Zhao, Kelvin Guu, Adams Wei Yu, Brian Lester, Nan Du, Andrew Mingbo Dai, and Quoc V. Le. Finetuned language models are zero-shot learners. 2022. URL https://openreview.net/forum?id=gEZrGCozdqR.

Haoran Zhang, Amy X. Lu, Mohamed Abdalla, Matthew McDermott, and Marzyeh Ghassemi. Hurtful words: Quantifying biases in clinical contextual word embeddings. In *Proceedings of the ACM Conference on Health, Inference, and Learning*, CHIL '20, page 110–120, New York, NY, USA, 2020. Association for Computing Machinery. ISBN 9781450370462. doi: 10.1145/3368555.3384448. URL https://doi.org/10.1145/3368555.3384448.

Appendix A. Hand-crafted Feature Queries for Chest X-ray Dataset

Table A.1: Features grouped by the labels they may support. (Features may be written under more than one label.)

No Finding	
normal	Is this patient normal?
clear lungs	Does this patient have clear lungs?
normal cardiac silhouette	Does this patient have a normal cardiac silhouette?
sharp costophrenic angles	Does this patient have sharp costophrenic angles?
Enlarged Cardiomediastinum	
enlarged cardiomediastinal silhouette	Does this patient have an enlarged cardiomediastinal silhouette?
Cardiomegaly	
enlarged cardiomediastinal silhouette	Does this patient have an enlarged cardiomediastinal silhouette?
increased cardiothoracic ratio	Does this patient have an increased cardiothoracic ratio?
prominent right atrial contour	Does this patient have a prominent right atrial contour?
enlarged heart	Does this patient have an enlarged heart?
globular cardiac silhouette	Does this patient have a globular cardiac silhouette?
rounded left heart border	Does this patient have a rounded left heart border?
uplifted cardiac apex	Does this patient have an uplifted cardiac apex?
double density	Does this patient have a double density?
splaying of carina	Is there splaying of the carina?
increase subcarinal angle	Does this patient have an increased subcarinal angle?
convex left atrial appendage	Does this patient have a convex left atrial appendage?
third mogul sign	Does this patient have a third mogul sign?
superior displacement of left mainstem bronchus	Does this patient have superior displacement of left mainstem bronchus?
rounded cardiac apex	Does this patient have a rounded cardiac apex?
shmoo sign	Does this patient have a shmoo sign?
hoffman rigler sign	Does this patient have a Hoffman-Rigler sign?
Edema	
upper lobe pulmonary venous engorgement	Does this patient have upper lobe pulmonary venous engorgement?
stags antler sign	Does this patient have a stag's antler sign?
bilateral opacity	Does this patient have bilateral opacity?
symmetric perihilar opacity	Does this patient have a symmetric perihilar opacity?
bat wing opacity	Does this patient have a bat wing opacity?
enlarged cardiac silhouette	Does this patient have an enlarged cardiac silhouette?
increased cardiothoracic ratio	Does this patient have an increased cardiothoracic ratio?
peribronchiolar cuffing	Does this patient have peribronchiolar cuffing?
hazy perihilar opacity	Does this patient have a hazy perihilar opacity?
septal thickening	Does this patient have septal thickening?
kerley b lines	Does this patient have Kerley B lines?
thickening of the fissures	Is there a thickening of the fissures?

fluid in the fissures	Does this patient have fluid in the fissures?
pleural effusion	Does this patient have a pleural effusion?
Pneumonia	
reticular opacity	Does this patient have a reticular opacity?
hazy opacity	Does this patient have a hazy opacity?
consolidation	Does this patient have consolidation?
segmental opacity	Does this patient have a segmental opacity?
lobar opacity	Does this patient have a lobar opacity?
bulging fissures	Does this patient have bulging fissures?
cavitation	Does this patient have cavitation?
Atelectasis	
subsegmental linear basilar opacity	Does this patient have a subsegmental linear basilar opacity?
linear basilar opacity	Does this patient have a linear basilar opacity?
subsegmental crescentic basilar opacity	Does this patient have a subsegmental crescentic basilar opacity?
crescentic basilar opacity	Does this patient have a crescentic basilar opacity?
decreased lung volumes	Does this patient have decreased lung volumes?
indistinct basilar opacity	Does this patient have indistinct basilar opacities?
Pneumothorax	
apical lucency	Does this patient have an apical lucency?
peripheral lucency	Does this patient have a peripheral lucency?
collapse of lung	Is there a collapse of a lung?
visible visceral pleura	Does this patient have visible visceral pleura?
Fracture	
lucency in a rib or clavicle	Does this patient have a lucency in a rib or clavicle?
deformity of a rib or clavicle	Does this patient have a deformity of a rib or clavicle?
wedge deformity of a vertebra	Does this patient have a wedge deformity of a vertebra?
step off of a rib or clavicle	Does this patient have a step-off of a rib or clavicle?
Lung Lesion	
rounded opacity	Does this patient have a rounded opacity?
pulmonary calcification	Does this patient have an pulmonary calcification?
cavitation	Does this patient have cavitation?
abnormal high density	Does this patient have an abnormal high density?
opacity with indistinct borders	Does this patient have an opacity with indistinct borders?
spiculated opacity	Does this patient have a spiculated opacity?
hazy opacity	Does this patient have a hazy opacity?
Lung Opacity	
alveolar blood	Is there alveolar blood?
alveolar fluid	Is there alveolar fluid?
Pleural Other	
pleural empyema	Is there pleural empyema?
hemothorax	Does the patient have hemothorax?
pleural tumor	Is there pleural tumor?
pleural thickening	Is there pleural tumor?
calcificied pleural plaques	Does this patient have a calcified pleural plaque?
foreign body in pleural space	Is there a foreign body in the pleural space?

Support Devices	
surgical clip	Does this patient have a surgical clip?
metallic density	Does this patient have a metallic density?
curvilinear density	Does this patient have a curvilinear density?
foreign body	Does this patient have a foreign body?
metal lead	Does this patient have a metal lead?
wire	Does this patient have a wire?
tube	Does this patient have a tube?
stent	Does this patient have a stent?
endotracheal tube	Does this patient have an endotracheal tube?
chest tube	Does this patient have a chest tube?
central venous catheters	Does this patient have a central venous catheter?
picc line	Does this patient have a PICC line?
tracheal stent	Does this patient have a tracheal stent?
coronary stent	Does this patient have a coronary stent?
aortic stent	Does this patient have an aortic stent?
arterial stent	Does this patient have an arterial stent?
pacemaker	Does this patient have a pacemaker?
icd	Does this patient have an ICD?
aortic balloon pump	Does this patient have an aortic balloon pump?
lvad	Does this patient have an lvad?
clamshell closure device	Does this patient have a clamshell closure device?
SVC stent	Does this patient have an SVC stent?
IVC stent	Does this patient have an IVC stent?
IVC filter	Does this patient have an IVC filter?
Other Features	
alveolar hemorrhage	Is there alveolar hemorrhage?
dense op air filling with pus water blood	Does this patient have a dense opacity that suggests the airspace filling with pus, water, or blood?
esophageal tube	Does this patient have an esophageal tube?
g-tube	Does this patient have a g-tube?
gastric tube	Does this patient have a gastric tube?
loculated pleural effusion	Is there a loculated pleural effusion?
nasogastric tube	Does this patient have a nasogastric tube?

	Phenotyping	Readmission	Mortality	Chest X-ray
BERT	0.820	0.661	0.874	0.992
TF-IDF (30)	0.624	0.573	0.692	0.753
TF-IDF (100)	0.697	0.613	0.787	0.874
TF-IDF (1k)	0.813	0.668	0.863	0.952
TF-IDF (30k)	0.830	0.694	0.872	0.953
Ground Truth	0.798	0.645	0.697	-
Inferred Binary	0.651	0.589	0.699	-
Inferred Binary w/ Custom	0.669	0.603	0.719	0.811
Inferred Continuous	0.705	0.614	0.752	-
Inferred Continuous w/ Custom	0.719	0.626	0.806	0.877
Zero-Shot Downstream	0.711	0.579	0.816	0.774

Table B.1: Expanded results of Downstream Classification Performance.

	Chest X-ray	Mortality	Phenotype	Readmission
TF-IDF (30)	1.98	1.00	3.05	3.41
TF-IDF (100)	1.79	2.67	3.84	4.54
TF-IDF (1k)	1.86	6.24	4.63	6.84
TF-IDF (30k)	4.17	10.27	9.50	10.30
Ground Truth	-	2.00	1.30	2.39
Inferred Binary	-	1.85	1.96	2.39
Inferred Binary w/ Custom	3.98	1.50	2.03	2.56
Inferred Continuous	-	1.97	1.65	2.31
Inferred Continuous w/ Custom	3.08	1.13	1.75	2.51

Table B.2: **How is the magnitude mass distributed across coefficients?** We report the **entropy** of the distribution described by the coefficient magnitudes: $H(\text{softmax}(|\boldsymbol{c}|)$ where $\boldsymbol{c}$ represents the vector of coefficients for a model. (Entropy is averaged over labels in the case of Phenotype and Chest X-ray tasks.) This measure gives some insight into how uniform the coefficient magnitudes are. TF-IDF (30k) has much higher entropy across the board indicating that many more features have high magnitude in this model.

Appendix B. Extra Figures and Tables

Table B.3: **AUC per Phenotyping label.**

	BERT	TF-IDF (30k)	Ground Truth	Inferred Continuous	Inferred Continuous w/ Custom	Zero-Shot Downstream
Conduction Disorders	0.856	0.847	0.712	0.678	0.676	0.758
Pneumonia (Except That Caused By Tuberculosis Or Sexually Transmitted Disease)	0.809	0.834	0.744	0.709	0.713	0.733
Disorders Of Lipid Metabolism	0.785	0.763	1.000	0.705	0.723	0.639
Acute Myocardial Infarction	0.867	0.862	0.785	0.788	0.796	0.805
Other Lower Respiratory Disease	0.696	0.719	0.684	0.580	0.630	0.649
Pleurisy; Pneumothorax; Pulmonary Collapse	0.663	0.722	0.583	0.593	0.627	0.661
Any-Chronic	0.874	0.867	0.951	0.779	0.784	0.659
Diabetes Mellitus With Complications	0.863	0.867	0.652	0.774	0.776	0.831
Cardiac Dysrhythmias	0.846	0.838	0.905	0.797	0.799	0.793
Any-Acute	0.819	0.834	0.819	0.715	0.726	0.515
Coronary Atherosclerosis And Other Heart Disease	0.870	0.868	0.964	0.820	0.838	0.801
Hypertension With Complications And Secondary Hypertension	0.873	0.870	0.864	0.749	0.769	0.670
Septicemia (Except In Labor)	0.874	0.883	0.748	0.732	0.728	0.782
Respiratory Failure; Insufficiency; Arrest (Adult)	0.882	0.884	0.985	0.787	0.784	0.780
Any-Disease	0.903	0.897	0.934	0.812	0.826	0.632
Congestive Heart Failure; Nonhypertensive	0.837	0.830	0.979	0.767	0.770	0.704
Chronic Obstructive Pulmonary Disease And Bronchiectasis	0.777	0.789	0.670	0.658	0.670	0.716
Complications Of Surgical Procedures Or Medical Care	0.712	0.756	0.589	0.569	0.581	0.701
Acute And Unspecified Renal Failure	0.830	0.848	0.956	0.703	0.714	0.646
Shock	0.873	0.872	0.756	0.715	0.726	0.694
Other Upper Respiratory Disease	0.831	0.833	0.642	0.686	0.698	0.737
Fluid And Electrolyte Disorders	0.734	0.760	0.691	0.648	0.650	0.618
Other Liver Diseases	0.828	0.855	0.661	0.641	0.669	0.730
Gastrointestinal Hemorrhage	0.855	0.887	0.583	0.628	0.636	0.779
Diabetes Mellitus Without Complication	0.700	0.723	0.971	0.719	0.720	0.638
Acute Cerebrovascular Disease	0.907	0.936	0.677	0.628	0.709	0.841
Essential Hypertension	0.729	0.720	0.996	0.627	0.634	0.588
Chronic Kidney Disease	0.857	0.869	0.830	0.736	0.771	0.817

Table B.4: **AUC per CheXpert label.**

	BERT	TF-IDF (30k)	Inferred Continuous w/ Custom	Zero-Shot Downstream
Atelectasis	0.997	0.968	0.888	0.944
Cardiomegaly	0.997	0.957	0.913	0.876
Edema	0.997	0.961	0.910	0.954
Enlarged Cardiom.	0.988	0.904	0.764	0.592
Support Devices	0.996	0.965	0.925	0.826
Pneumothorax	0.990	0.950	0.911	0.868
Fracture	0.999	0.987	0.948	0.977
Pneumonia	0.982	0.921	0.795	0.799
Pleural Other	0.995	0.965	0.804	0.566
No Finding	0.987	0.944	0.906	0.230
Lung Opacity	0.994	0.944	0.899	0.858
Lung Lesion	0.976	0.965	0.862	0.804

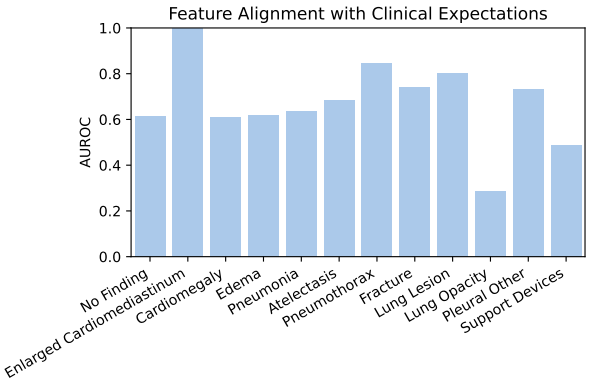

Figure B.1: Using a set of features annotated as supporting a particular label, we plot the AUROC obtained by using the coefficient values (from the continuous features model) to predict this feature list for each label.

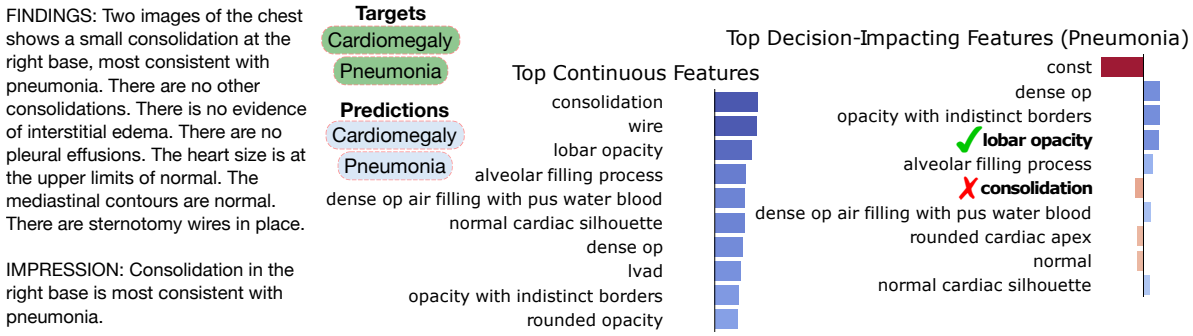

Figure B.2: Qualitative Example of Features and Feature Influence for Pneumonia. (Similar to Figure 7.) This seems to correctly predict Pneumonia, but this happens in spite of consolidation being incorrectly identified by the linear model as not supporting Pneumonia. These plots make clear that this is not a mistake of the feature extractor at inference time because consolidation is among the top Features. The mistake comes from the linear model having a negative coefficient for consolidation.